



HAL
open science

Heteroleptic diimine copper(i) complexes with large extinction coefficients: synthesis, quantum chemistry calculations and physico-chemical properties.

Martina Sandroni, Megumi Kayanuma, Mateusz Rebarz, Huriye Akdas-Kilig, Yann Pellegrin, Errol Blart, Hubert Le Bozec, Chantal Daniel, Fabrice Odobel

► To cite this version:

Martina Sandroni, Megumi Kayanuma, Mateusz Rebarz, Huriye Akdas-Kilig, Yann Pellegrin, et al.. Heteroleptic diimine copper(i) complexes with large extinction coefficients: synthesis, quantum chemistry calculations and physico-chemical properties.. Dalton Transactions, 2013, 42 (40), pp.14628-14638. 10.1039/c3dt51288f. hal-00861248

HAL Id: hal-00861248

<https://hal.science/hal-00861248>

Submitted on 12 Sep 2013

HAL is a multi-disciplinary open access archive for the deposit and dissemination of scientific research documents, whether they are published or not. The documents may come from teaching and research institutions in France or abroad, or from public or private research centers.

L'archive ouverte pluridisciplinaire **HAL**, est destinée au dépôt et à la diffusion de documents scientifiques de niveau recherche, publiés ou non, émanant des établissements d'enseignement et de recherche français ou étrangers, des laboratoires publics ou privés.

Heteroleptic diimine copper (I) complexes with large extinction coefficients: synthesis, quantum chemistry calculations and physico-chemical properties

Martina Sandroni,^a Megumi Kayanuma,^b Mateusz Rebarz,^c Huriye Akdas-Kilig,^d Yann Pellegrin,^a Errol Blart,^a Hubert Le Bozec,^d Chantal Daniel,^{b*} Fabrice Odobel^{a*}

^aUniversité UNAM, Université de Nantes, CNRS, Chimie et Interdisciplinarité: Synthèse, Analyse, Modélisation (CEISAM), UMR 6230, 2, rue de la Houssinière – BP 92208 – 44322 Nantes Cedex 3, France. Tel: +33 (0)2 51 12 54 29. Fax: +33 (0)2 51 12 54 02. E-mail: Fabrice.Odobel@univ-nantes.fr.

^bLaboratoire de Chimie Quantique Institut de Chimie UMR 7177 CNRS-Université de Strasbourg, 4 Rue Blaise Pascal CS 90032 F-67081 Strasbourg Cedex. E-mail: c.daniel@unistra.fr; Fax: +33 368851589; Tel. +33 368 851314

^cLaboratoire de Spectrochimie Infrarouge et Raman CNRS 8516 Université Lille Nord de France, Université Lille 1 Sciences et Technologies, 59655 Villeneuve d'Ascq Cedex, France. E-mail : michel.sliwa@univ-lille1.fr

^dUMR CNRS 6226-Université de Rennes 1, Sciences Chimiques de Rennes, Campus de Beaulieu, 35042 Rennes Cedex, France. .

Abstract

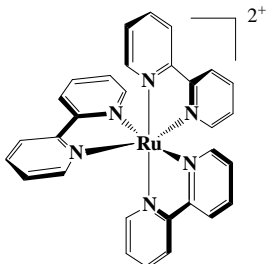
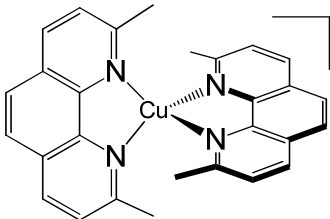
Using the HETPHEN approach, five new heteroleptic copper(I) complexes composed of a push-pull 4,4'-styryl-6,6'-dimethyl-2,2'-bipyridine ligand and a bulky Bis[(2-diphenylphosphino)phenyl]-ether (DPEphos) or a bis(2,9-mesityl phenanthroline) (Mes₂Phen) were prepared and characterized by electronic absorption spectroscopy, electrochemistry, and TD-DFT calculations were performed. These complexes exhibit indeed very intense absorption bands in the visible region with extinction coefficient in the range $5\text{-}7 \times 10^4 \text{ M}^{-1}\text{cm}^{-1}$. The analysis of the position, intensity and band shape indicates a strong contribution of an intra-ligand charge-transfer transition centered on the styrylbipyridine ligand along with MLCT transitions. These new complexes experimentally demonstrate that large light harvesting properties with bis-diimine copper(I) complexes showed is a reality if one chooses suitable ligands in the coordination sphere. This constitutes a milestone to use bis-diimine copper(I) complexes for solar energy conversion (artificial photosynthesis and solar cells).

Introduction

The supramolecular chemistry of transition-metal polypyridine complexes is dominated by ruthenium trisbipyridine complexes and its derivatives.¹ The reasons of this success lie in: i) their long-lived metal-to-ligand charge transfer (MLCT) excited states, ii) significant light absorption in the visible region, iii) intense emission, iv) high photochemical and electrochemical stability and v)

synthetic versatility. Other metal complexes also display such valuable electronic properties such as those with osmium(II),² platinum(II),³ iridium(III)⁴ and rhenium(I).⁵ However, these metals are noxious and relatively expensive as they are not very abundant in the earth's crust. An appealing alternative is copper, because diimine copper(I) complexes also exhibit MLCT excited states in the visible region^{6, 7} and copper is much cheaper, more abundant and less toxic than the above mentioned precious metals. A quick comparison of the photophysical properties of the widely used $[\text{Ru}(\text{bpy})_3]^{2+}$ and those of $[\text{Cu}(\text{dmp})_2]^+$ (dmp = 2,9-dimethyl-1,10-phenanthroline) shows that they are quite similar except that the latter has a lower extinction coefficient on the MLCT absorption band, a shorter-lived emission and a lower luminescence quantum yield than the former (Table 1). These differences are quite general between copper(I) bis-diimine and ruthenium(II) trisbipyridine complexes.

Table 1. Summary of some characteristics of ruthenium(II) trisbipyridine and copper(I) bis 2,9-dimethyl phenanthroline.

		
Abundance on earth	Ru: 0.001 ppm	Cu: 60 ppm
Photophysical properties	$\lambda_{\text{abs}} = 450 \text{ nm}$ $(\epsilon = 1.5 \times 10^4 \text{ M}^{-1}\text{cm}^{-1})$ $\lambda_{\text{em}} = 650 \text{ nm}$ ($\tau_{\text{em}} = 850 \text{ ns}$ in degassed CH_3CN) $E_{00} = 2.1 \text{ eV}$	$\lambda_{\text{abs}} = 460 \text{ nm}$ $(\epsilon = 0.8 \times 10^4 \text{ M}^{-1}\text{cm}^{-1})$ $\lambda_{\text{em}} = 750 \text{ nm}$ ($\tau_{\text{em}} = 90 \text{ ns}$ in degassed CH_2Cl_2) $E_{00} = 2.0 \text{ eV}$

The short lifetime of the MLCT emission of most copper(I) diimine complexes stems from the photoinitiated Jahn-Teller distortions that result in a structural rearrangement from a nearly tetrahedral ground state to a square planar or trigonal bipyramidal excited state which non-radiatively deactivates by forming a pentacoordinated exciplex.^{6, 7} The formation of a pyramidal pentacoordinated complex results from the square planar preference of Cu(II), a d^9 cation. However, it has been shown^{8, 9} that bulky substituents in the 2 and 9 positions of the diimine ligand inhibit the molecular distortion that occurs in the MLCT excited state and this leads to large improvements of the excited-state lifetime and emission quantum yield, which respectively reach values as large as 3.2 μs and 5.6 % for the completely locked bis(2,9-di-tert-butyl-1,10-phenanthroline)copper(I) complex.^{10, 11}

The goal of the present work was to develop new copper(I) complexes exhibiting higher absorption coefficients on the main absorption band to optimize the visible absorption cross-section. Indeed, the presence of intense absorption bands in the visible spectrum is a valuable property in view of using these complexes for practical applications such as solar energy conversion, light emitting diode¹²⁻¹⁴ and luminescent sensing probe.^{15, 16} In particular for solar energy conversion, the development of copper-based sensitizers for dye-sensitized solar cells,¹⁷⁻²⁷ molecular arrays for photoinduced charge separation^{28, 29} or photocatalysis^{21, 30} demand highly absorbing dyes. To achieve this goal, we decided to use the HETPHEN strategy developed by Schmittl and co-workers^{25, 31} to build stable heteroleptic complexes and we incorporated a bipyridine ligand presenting an extended π -conjugation in the coordination sphere of copper. Such π -conjugated chromogenic ligands were previously used to prepare ruthenium polypyridine complexes and they proved to be suitable to strongly enhance the absorbance in the visible region.^{32, 33} In a second objective, we explore the influence of different coordination patterns around the copper cation by completing the styryl bipyridine ligand with two different bulky bidentate ligands, either a bis[2-(diphenylphosphino)phenyl]-ether (DPEphos) or a 2,9-dimesityl-1,10-phenanthroline (Mes₂Phen) (Figure 1). Indeed, DPEphos complexes with copper(I) were reported to be particularly luminescent^{7, 34, 35} while Mes₂Phen provides an easy entry towards more functionalized complexes as the substitution on this type of ligands is quite straightforward. This spectator ligand also opens the opportunity to introduce new functions such as anchoring groups (to graft on surfaces or to label proteins) or electron donors or acceptors. Moreover, electron releasing substituents of different strength were also introduced on the styryl bipyridine ligand to tune the energy of the frontier molecular orbitals of this ligand and to assess their impact on the photophysical properties of the complexes. In this work, we report the synthesis of the new highly absorbing copper(I) complexes **C1-C5** (Figure 1) and analyze in details their absorption properties and electronic structure through spectroscopic and electrochemical measurements as well as TD-DFT calculations.

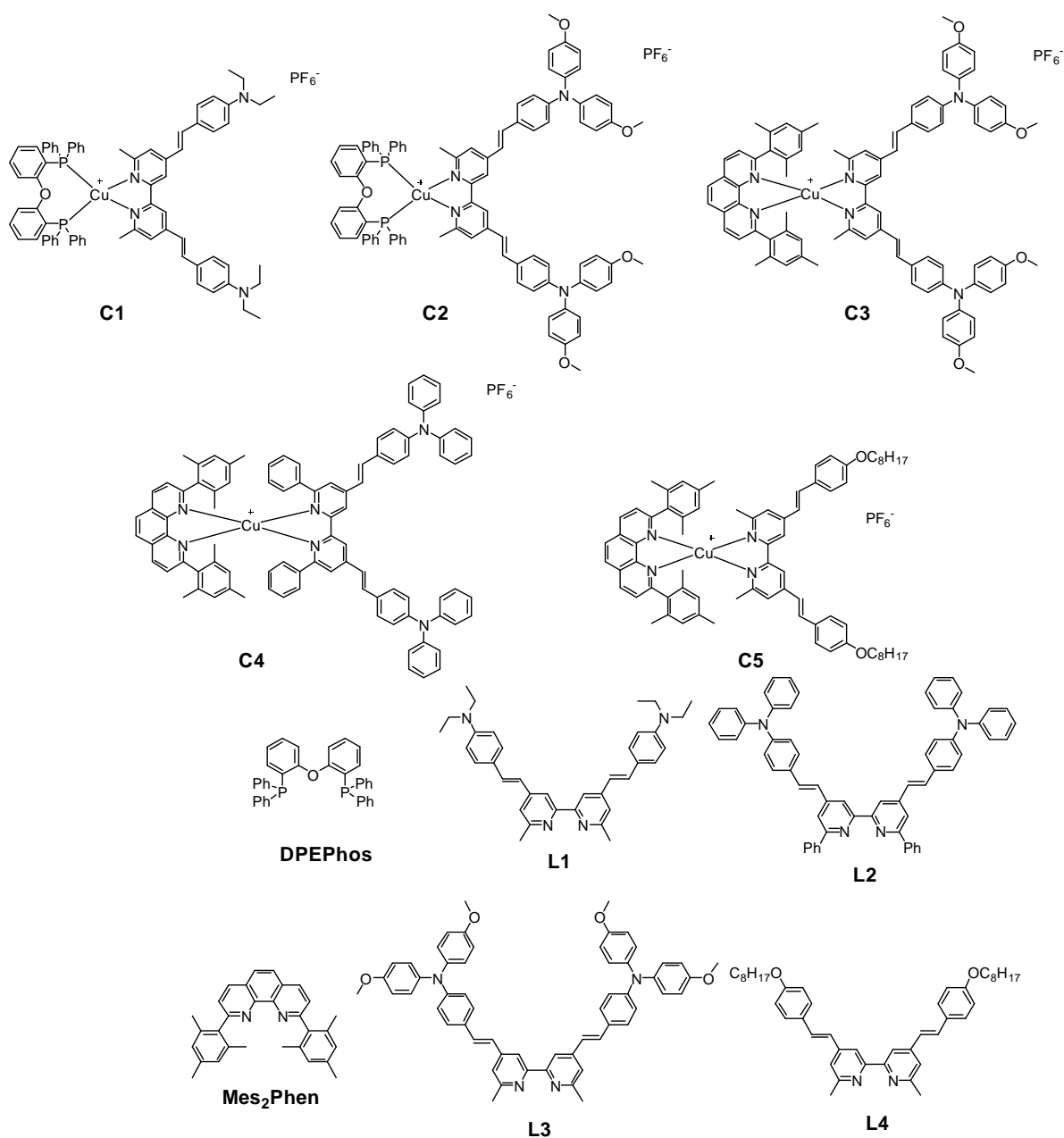


Figure 1. Structure of the complexes and of the ligands described in this study.

Experimental section

General procedures

Reagents and solvents

Ligands **L1**,²⁴ **L2**,²² 4,4',6,6'-tetramethyl-2,2'-bipyridine,²⁶ 2,9-dimesityl-1,10-phenanthroline (**Mes₂Phen**)³⁶ 4,4'-methylphosphonateethyl ester-6,6'-dimethyl-2,2'-bipyridine,¹⁵⁻³⁷ 4-di(4'-methoxyphenyl)aminobenzaldehyde³⁸, and the starting complex [Cu(MeCN)₄]PF₆³⁹ were prepared according to literature procedures.

¹H and ¹³C-NMR spectra were recorded on an ARX 300 MHz or AMX 400 MHz Bruker spectrometer (the instrument is specified for every molecule). Chemical shifts are referenced relative to the residual protium in the deuterated solvent.

MALDI-TOF analyses were performed on an Applied Biosystems Voyager DE-STR spectrometer, positive linear mode at 20 kV acceleration voltage with DHB/CH₃CN (DHB: 2,5-dihydroxybenzoic acid) or dithranol/CH₃CN as matrix.

UV-Visible spectra were recorded in analytically pure solvents, with a UV 2501PC Shimadzu spectrophotometer. Beer Lamber law was respected in the conditions of the UV-Vis. spectrum recording, therefore the degree of aggregation is inexistent or weak. Electrochemistry measurements were performed with an Autolab PGSTAT 302N potentiostat in freshly distilled dichloromethane, with a platinum disk working electrode, a platinum foil counter electrode and a saturated calomel reference electrode (SCE). All potentials are referenced vs. SCE. In our conditions the Fc⁺/Fc couple was found at 0.45 V vs. SCE. The measurements were conducted at the concentration of *ca* 1 mMol/L in dichloromethane with 0.1 N of n-Bu₄NPF₆ as supporting electrolyte. The solution was purged with argon before the measurements. In all the experiments the scan rate was 100 mV/s.

4,4'-dianisylaminostyryl-6,6'-dimethyl-2,2'-bipyridine (L3)

In a Schlenk flask, 4,4'-methylphosphonateethyl ester-6,6'-dimethyl-2,2'-bipyridine **4** (300 mg, 6.22.10⁻⁴ mol) and 4-dianisylaminobenzaldehyde (517 mg, 1.55 mmol, 2.5 equiv.) were dissolved in THF (10 mL) and tBuOK (348 mg, 3.11 mmol) was slowly added at room temperature. The solution, which immediately turned brown, was then stirred for 3 h. Addition of water led to the formation of a pale precipitate, which was filtered. The crude solid was purified by column chromatography on silica gel (eluant CH₂Cl₂: AcOEt = 90:10 → 85: 15) to afford pure **L3** (227 mg, 43%).

¹H-NMR (300 MHz, CDCl₃, 25 °C): δ = 8.24 (s, 2H), 7.38-7.32 (m, 6H), 7.22 (s, 2H), 7.09 (d, 8H, J = 8.7 Hz), 6.89-6.95 (m, 6H), 6.85 (d, 8H, J = 9 Hz), 3.81 (s, 12H), 2.66 (s, 6H) ppm.

¹³C-NMR (75 MHz, CDCl₃, 25 °C): δ = 158.23, 156.52, 156.29, 149.24, 146.41, 140.53, 132.60, 128.47, 127.94, 127.07, 123.66, 120.04, 119.95, 115.74, 114.89, 55.63, 24.85 ppm.

HR-MS (MALDI): m/z = 843.3900 [M+H]⁺ (calculated for [M-H]⁺ = 843.3905).

4,4'- p-octyloxystyryl-6,6'-dimethyl-2,2'-bipyridine (L4)

By the same procedure as described for **L3**, compound **L4** was isolated from 4,4'-methylphosphonateethyl ester-6,6'-dimethyl-2,2'-bipyridine **4** (200 mg, 4.13.10⁻⁴ mol), 4-octyloxybenzaldehyde (387 mg, 1.65 mmol, 4 equiv.) and tBuOK (185 mg, 1.65 mmol) in THF (10ml) as a creamy solid (170 mg, 64 %).

¹H-NMR (400 MHz, CDCl₃, 25 °C): δ = 8.30 (s, 2H), 7.50 (d, J = 8.5 Hz, 4H), 7.38 (d, J = 16.31 Hz, 2H), 7.24 (s, 2H), 6.98 (d, J = 16.31 Hz, 2H), 6.92 (d, J = 8.5 Hz, 4H), 3.99 (t, J = 6.5 Hz, 4H), 2.68 (s, 6H), 1.81 (m, 4H), 1.48 (m, 4H), 1.31 (m, 16H), 0.90 (m, 6H) ppm.

¹³C-NMR (100 MHz, CDCl₃, 25 °C): δ = 159.63, 158.18, 156.43, 146.14, 132.40, 129.11, 128.32, 124.28, 120.06, 115.65, 114.82, 68.14, 31.84, 29.39, 29.27, 26.07, 24.73, 22.69, 14.13 ppm.

HR-MS (MALDI): m/z = 645.4438 [M+H]⁺ (calculated for [M-H]⁺ = 645.4415).

Elemental analysis: Calculated for C₄₄H₅₆N₂O₂: C, 81.94; H, 8.75; N, 4.34. Found: C, 81.79; H, 8.76; N, 4.41.

[Cu(DPEphos)(L1)]PF₆ (C1)

[Cu(MeCN)₄]PF₆ (45 mg, 0.12 mmol) and DPEphos (65 mg, 0.12 mmol) were stirred in 5 mL of distilled dichloromethane at room temperature for 10 minutes under Ar atmosphere, then 4 mL of a degassed solution of **L1** (57 mg, 0.11 mmol) in dichloromethane were injected under Ar and the resulting deep red solution was stirred for further 30 minutes at room temperature. The solvent was removed under reduced pressure and the resulting dark red solid was purified by column chromatography on silica gel (CH₂Cl₂: CH₃OH = 100: 0 → 92: 8, medium pressure chromatography) to afford 65 mg (46%) of pure **C1**.

¹H-NMR (500 MHz, acetone-d₆, 25 °C): δ = 8.39 (d, 2H, J = 1 Hz), 7.64 (d, 2H, J = 16.5 Hz), 7.54 (d, 4H, J = 8.5 Hz), 7.47 (d, 2H, J = 1.5 Hz), 7.44 (m, 2H), 7.36 (tm, 4H), 7.29 (tm, 2H), 7.27-7.22 (m, 10H), 7.19-7.14 (m, 8H), 7.03 (dm, 2H), 7.02 (d, 2H, J = 16.5 Hz), 6.79 (d, 4H, J = 9.0 Hz), 3.46 (q, 8H, J = 6.9 Hz), 2.26 (s, 6H), 1.18 (t, 12H, J = 6.9 Hz) ppm.

¹³C-NMR (75 MHz, acetone-d₆, 25 °C): δ = 159.05, 153.99, 149.69, 136.94, 134.47, 134.13, 134.04, 133.94, 132.98, 132.77, 130.77, 130.01, 129.55, 126.45, 126.27, 126.09, 123.88, 122.73, 120.99, 120.12, 119.66, 117.43, 112.42, 44.96, 26.79, 12.89 ppm.

HR-MS (ESI⁺): m/z = 1131.4266 (calculated for [M-PF₆]⁺ = 1131.4315).

Elemental analysis: Calculated for C₇₂H₇₀CuF₆N₄OP₃ · 0.75 CH₂Cl₂: C, 65.13; H, 5.37; N, 4.18. Found: C, 64.93; H, 5.19; N, 4.18.

[Cu(DPEphos)(L3)]PF₆ (C2)

[Cu(MeCN)₄]PF₆ (9.3 mg, 0.025 mmol) and DPEphos (17 mg, 0.031 mmol) were stirred in 5 mL of distilled dichloromethane at room temperature for 15 minutes under Ar atmosphere, then 2 mL of a degassed solution of **L3** (21 mg, 0.024 mmol) in dichloromethane were injected under Ar and the resulting orange solution was stirred for further 30 minutes at room temperature. The solvent was removed under reduced pressure and the resulting orange solid was purified first by column

chromatography on alumina (CH_2Cl_2) and then by size exclusion chromatography on Sephadex LH20 (acetone) to afford 28 mg (72%) of pure **C2**.

$^1\text{H-NMR}$ (400 MHz, acetone- d_6 , 25 °C): δ = 8.40 (s, 2H), 7.64 (d, 2H, J = 16.4 Hz), 7.51 (s, 2H), 7.49 (d, 4H, J = 8.8 Hz), 7.42 (tm, 2H), 7.34 (tb, 4H, J = 7.2 Hz), 7.30-7.20 (m, 12H), 7.17-7.08 (m, 18H), 7.10 (dm, 2H), 6.95 (d, 8H, J = 9.2 Hz), 6.84 (d, 4H, J = 8.8 Hz), 3.81(s, 12H), 2.29 (s, 6H) ppm.

$^{13}\text{C-NMR}$ (100 MHz, acetone- d_6 , 25 °C): δ = 159.30, 159.05, 157.87, 154.04, 151.01, 149.26, 140.82, 136.26, 134.52, 134.13, 134.05, 133.97, 133.18, 133.11, 132.96, 132.80, 130.81, 129.58, 129.31, 128.37, 126.40, 126.13, 123.14, 122.20, 120.99, 119.51, 117.89, 115.84, 55.81, 26.81 ppm.

HR-MS (ESI+): m/z = 1443.47375 (calculated for $[\text{M-PF}_6]^+$ = 1443.47380).

Elemental analysis: Calculated for $\text{C}_{92}\text{H}_{78}\text{CuF}_6\text{N}_4\text{O}_5\text{P}_3 \cdot 0.90 \text{CH}_2\text{Cl}_2 \cdot 0.15 \text{H}_2\text{O}$: C, 66.85; H, 4.84; N, 3.36. Found: C, 66.95; H, 4.95; N, 3.24.

[Cu(Mes₂Phen)(L3)]PF₆ (C3)

$[\text{Cu}(\text{MeCN})_4]\text{PF}_6$ (10 mg, 0.027 mmol) and Mes₂Phen (13 mg, 0.032 mmol) were stirred in 8 mL of dry and degassed dichloromethane at room temperature for 15 minutes, then 5 mL of a degassed solution of **L3** (22 mg, 0.026 mmol) in dichloromethane were injected under Ar and the resulting deep red solution was stirred for further 30 minutes at room temperature. The solvent was removed under reduced pressure and the resulting red solid was purified by column chromatography on silica gel (CH_2Cl_2 : CH_3OH = 98: 2 \rightarrow 96: 4) to afford 26 mg (68%) of pure **C3**.

$^1\text{H-NMR}$ (300 MHz, CDCl_3 , 25 °C): δ = 8.67 (d, 2H, J = 8.4 Hz), 8.20 (s, 2H), 7.81 (d, 2H, J = 8.1 Hz), 7.78 (sb, 2H), 7.44 (d, 4H, J = 9.0 Hz), 7.38 (d, 2H, J = 16.2 Hz), 7.22 (sb, 2H), 7.10 (d, 8H, J = 9.0 Hz), 6.97 (d, 2H, J = 16.2 Hz), 6.92 (d, 4H, J = 8.7 Hz), 6.86 (d, 8H, J = 9.0 Hz), 6.41 (s, 4H), 3.82 (s, 12H), 1.99 (s, 6H), 1.91 (s, 6H), 1.69 (s, 12H) ppm.

HR-MS (MALDI): m/z = 1321.5351 (calculated for $[\text{M-PF}_6]^+$ = 1321.5375).

Elemental analysis: Calculated for $\text{C}_{86}\text{H}_{78}\text{CuF}_6\text{N}_6\text{O}_4\text{P} \cdot 0.75 \text{CH}_2\text{Cl}_2 \cdot 0.05 \text{H}_2\text{O}$: C, 67.98; H, 5.23; N, 5.48. Found: C, 67.98; H, 5.21; N, 5.49.

[Cu(Mes₂Phen)(L2)]PF₆ (C4)

$[\text{Cu}(\text{MeCN})_4]\text{PF}_6$ (8 mg, 0.021 mmol) and Mes₂Phen (11 mg, 0.026 mmol) were stirred in 5 mL of distilled dichloromethane at room temperature for 15 minutes under Ar atmosphere, then 3 mL of a degassed solution of **L2** (17 mg, 0.020 mmol) in dichloromethane were injected under Ar and the resulting red solution was stirred for further 30 minutes at room temperature. The solvent was removed under reduced pressure and the resulting red-orange solid was purified by size exclusion

chromatography on Sephadex LH20 (acetone) to afford 26 mg (87%) of pure **C4**. Use of silica gel was avoided because the complex seemed to degrade on TLC with releasing of ligand **L2**.

$^1\text{H-NMR}$ (300 MHz, acetone- d_6 , 25 °C): δ = 8.80 (d, 2H, J = 8.4 Hz), 8.55 (s, 2H), 8.28 (s, 2H), 7.89 (d, 2H, J = 16.5 Hz), 7.82 (m, 4H), 7.64 (d, 4H, J = 8.4 Hz), 7.40-7.32 (m, 14H), 7.15-7.12 (m, 12H), 7.04 (db, 6H), 6.77 (t, 4H, J = 7.8 Hz), 6.49 (s, 4H), 2.09 (s, 6H, partially superposed to the solvent peak), 1.42 (s, 12H) ppm.

$^{13}\text{C-NMR}$ (75 MHz, acetone- d_6 , 25 °C): δ = 160.60, 158.67, 155.61, 149.80, 148.30, 148.08, 145.07, 139.55, 138.84, 138.69, 137.40, 135.98, 135.83, 130.67, 130.46, 129.64, 129.39, 129.07, 128.50, 128.18, 125.97, 124.78, 123.65, 123.50, 122.95, 120.07, 21.15, 20.42 ppm.

HR-MS (MALDI): m/z = 1325.4243 (calculated for $[\text{M-PF}_6]^+$ = 1325.5265).

Elemental analysis: calculated for $\text{C}_{92}\text{H}_{74}\text{CuF}_6\text{N}_6\text{P} \cdot 0.55 \text{CH}_2\text{Cl}_2 \cdot 0.05 \text{H}_2\text{O}$: C, 73.14 ; H, 5.02 ; N, 5.53. Found: C, 73.06; H, 5.02; N, 5.62.

[Cu(Mes₂Phen)(L4)]PF₆ (C5)

$[\text{Cu}(\text{MeCN})_4]\text{PF}_6$ (17 mg, 0.045 mmol) and Mes₂Phen (21 mg, 0.051 mmol) were stirred in 4 mL of dry and degassed dichloromethane at room temperature for 15 minutes, then 4 mL of a degassed solution of **L4** (25 mg, 0.040 mmol) in dichloromethane were injected under Ar and the resulting deep red solution was stirred for further 30 minutes at room temperature. The solvent was removed under reduced pressure and the resulting red solid was purified by column chromatography on silica gel (CH_2Cl_2 : CH_3OH = 98: 2) to afford 42 mg (83%) of pure **C5**.

$^1\text{H-NMR}$ (300 MHz, acetone- d_6 , 25 °C): δ = 8.97 (d, 2H, J = 8.2 Hz), 8.41 (s, 2H), 8.28 (sb, 2H), 8.04 (d, 2H, J = 8.2 Hz), 7.72-7.64 (m, 6H), 7.50 (s, 2H), 7.18 (d, 2H, J = 16.3 Hz), 7.03 (d, 4H, J = 8.6 Hz), 6.48 (s, 4H), 4.07 (t, 4H, J = 6.5 Hz), 1.99 (s, 6H), 1.85-1.73 (m, 16H), 1.53-1.45 (m, 4H), 1.41-1.28 (m, 16H), 0.89 (t, 6H, J = 6.9 Hz) ppm.

$^{13}\text{C-NMR}$ (75 MHz, acetone- d_6 , 25 °C): δ = 161.18, 160.35, 157.44, 153.16, 147.86, 144.83, 138.89, 138.61, 137.88, 135.65, 135.40, 129.73, 129.65, 129.27, 128.45, 128.19, 127.93, 123.67, 122.72, 116.98, 115.87, 68.82, 32.57, 26.77, 25.92, 23.31, 21.08, 20.29, 14.34 ppm.

HR-MS (MALDI): m/z = 1123.5914 (calculated for $[\text{M-PF}_6]^+$ = 1123.5885).

Elemental analysis: Calculated for $\text{C}_{74}\text{H}_{84}\text{CuF}_6\text{N}_4\text{O}_2\text{P} \cdot 1.9 \text{H}_2\text{O}$: C, 68.15; H, 6.79; N, 4.30. Found: C, 67.83; H, 6.45; N, 4.25.

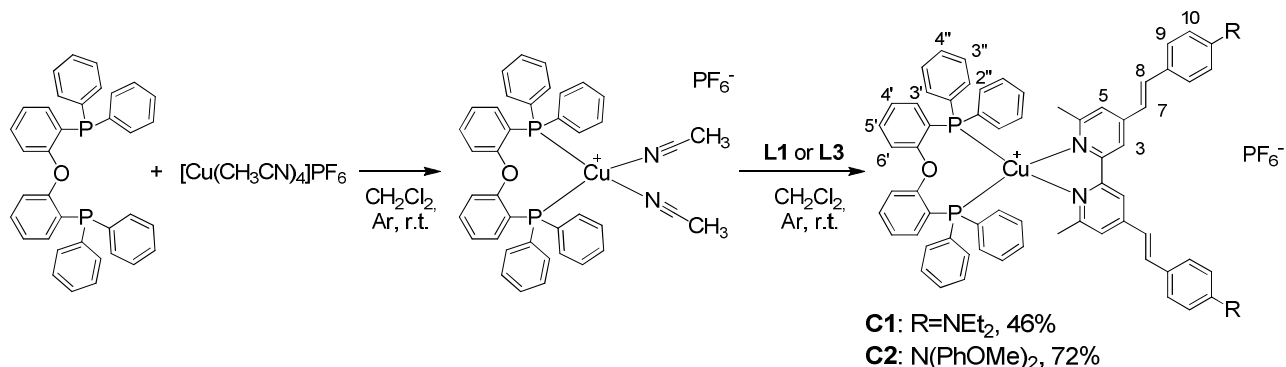
Computational chemistry: the geometries of complexes **C1** to **C5** in the ^1A electronic ground state have been optimized at the density functional theory (DFT) level using PBE-D functional (generalized gradient approximation PBE functional with Grimm's dispersion correction²⁹) and TZP basis sets⁴⁰ for all the atoms. These calculations have been performed under C_1 symmetry in

vacuum using ADF2010.02 quantum chemistry software.⁴¹ Although the PBE-D functional reproduces the structures of Cu complexes which have a π -stacking structure as shown in our previous studies,⁴² it is not adapted at describing planarity of floppy π -system and tends to make long ligands (L) curved. Therefore we added several constraints to keep L planar. The theoretical absorption spectra of complexes **C1-C5** have been calculated by means of time-dependent DFT (TD-DFT) method⁴³ using CAM-B3LYP functional⁴⁴ with solvent effect of dichloromethane at PBE-D optimized structures. Solvent effect was considered using Polarizable Continuum Model (PCM) using the integral equation formalism variant (IEFPCM).⁴⁵ The modified Ahlrichs TZV basis set (7s, 6p, 5d) contracted to [6s, 3p, 3d] for the Cu atom⁴⁶ and cc-pVDZ basis sets for the other atoms⁴⁷ have been used. TD-DFT calculations have been performed using a modified version of Gaussian 09 quantum chemistry software.⁴⁸

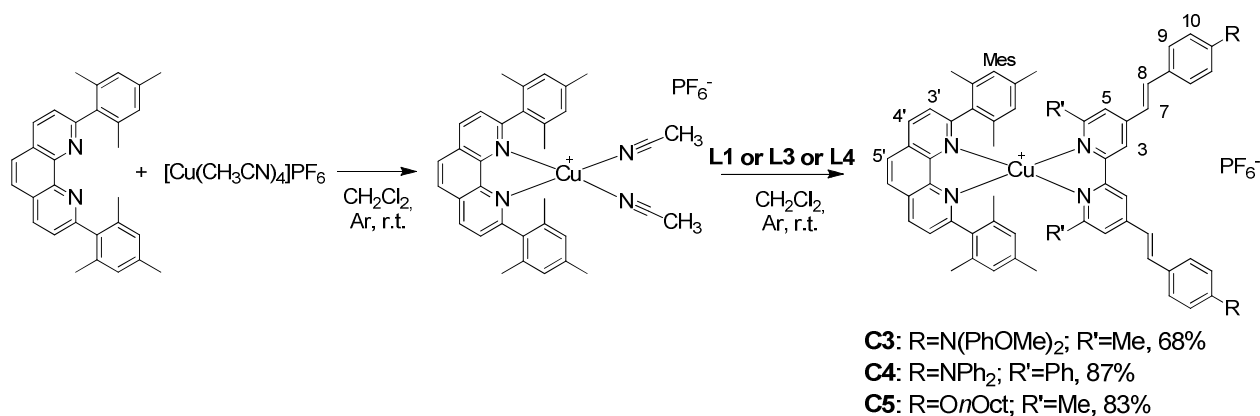
Results and discussion

Syntheses

Complexes **C1-C5** were prepared using the HETPHEN approach,^{25, 31} which allows the synthesis of stable heteroleptic structures despite the well-known lability of copper(I) complexes, which normally leads to a fast ligand scrambling in solution. This strategy is based on the combination of a bulky ligand (DPEphos or Mes₂Phen) with a less hindered one (6,6'-dimethyl-2,2'-bipyridine or 6,6'-diphenyl-2,2'-bipyridine). In a first step, a 1:1 complex was obtained by stirring the metallic precursor [Cu(MeCN)₄]PF₆ with DPEphos or Mes₂Phen, the formation of the 2:1 adduct being prevented at this stage by the steric hindrance around the copper. Then, the addition of the less hindered species (**L1-L4**) provided the heteroleptic complex in good yield (Schemes 1-2).



Scheme 1. Synthesis of complexes **C1** and **C2** with ligand **DPEphos**.



Scheme 2. Synthesis of complexes **C3-C5**.

Remarkably, the addition of the second ligand immediately induced a spontaneous intense colour change, which could be seen with the naked eye: the solution passed from colourless (or light yellow when Mes₂Phen was used) to deep orange or deep red, depending on the ligands. This fact is unusual for Cu-DPEPhos complexes, whose absorption in the visible is normally limited to a tail and are consequently only slightly coloured ($\lambda_{\text{max}} < 400$ nm). For copper diimine complexes, on the other hand, the MLCT band belongs to the visible region ($\lambda_{\text{max}} \sim 450$ nm) but the normal absorption coefficients are quite low and the solutions are not intensely colored. All the five copper (I) heteroleptic complexes are stable as solids and in solution and can be conserved under normal atmospheric conditions without degradation. Interestingly, the formation of a stable copper complex is observed even with the bulkier **L2** ligand despite the presence of the phenyl substituents on the 6 and 6' positions of the bipyridine, which prevents very close approach of the nitrogen to the copper cation to make strong bonds. Note however that partial dissociation of the complex **C4** was observed on silica gel thin layer chromatography (TLC), probably due to the above-mentioned high steric hindrance effect. On the other hand, the steric strains imposed by ligand **L2** are not compatible with the formation of a copper complex with the very bulky DPEphos ligand, which can also account for its instability during the purification. Analogous behaviour was previously reported in literature, where the attempt to prepare [Cu(DPEphos)(2,9-diphenyl-1,10-phenanthroline)]BF₄ failed, giving only [Cu(2,9-diphenyl-1,10-phenanthroline)₂] BF₄.³¹ All the new products were characterized by satisfying ¹H-NMR, ¹³C-NMR, HR-MS and elemental analyses.

UV-Vis absorption spectroscopy and quantum chemical calculations

The UV-Vis absorption spectra of ligands **L1-L4** and of complexes **C1-C5** recorded in dichloromethane are shown in Figures 2 and 3, respectively. The corresponding data are gathered in Table 2. The UV-Visible spectra of the four ligands are characterized by a strong absorption in the near UV with an extinction coefficient between 4 and 6 × 10⁴ M⁻¹cm⁻¹. Given the structure of these

ligands, this band can be assigned to an intra-ligand charge transfer (ILCT) transition resulting from an electron density shift from the donor moiety (amine or alkoxy group) to the bipyridine core.³²

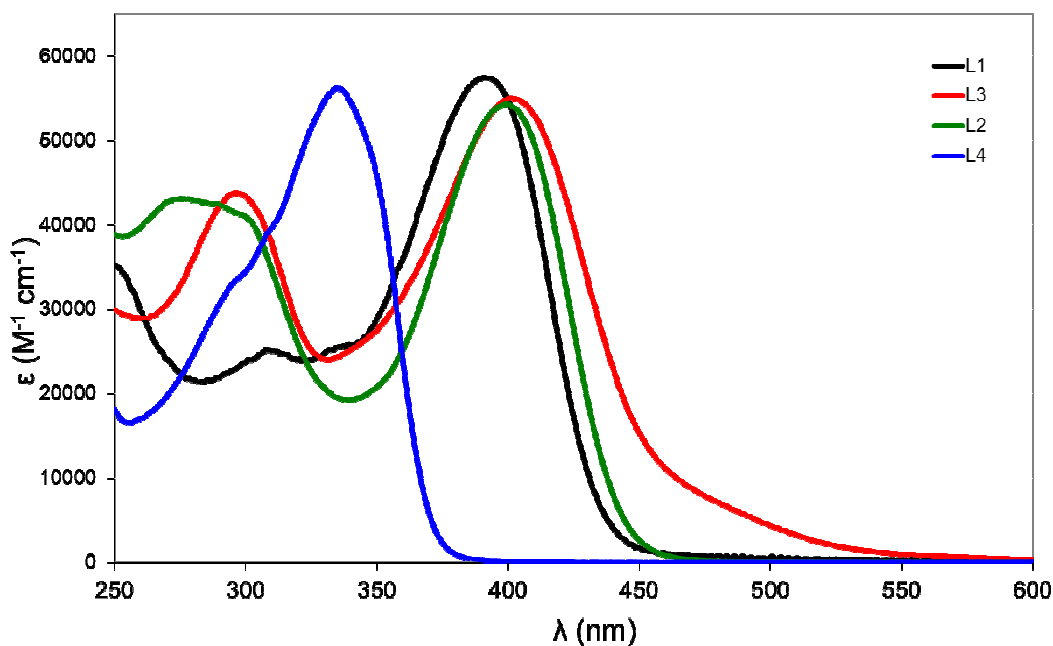


Figure 2. UV-Visible absorption spectra of the ligands **L1-L4**, recorded in dichloromethane.

The influence of the donor groups on the optical properties is well demonstrated by comparing **L1** and **L3** to **L4**. The first two ligands appear as yellow to orange powders and have an absorption maximum around 390-400 nm, with a tail in the visible region responsible for their color. Conversely, **L4** is a perfectly white powder as it does not absorb in the visible region (λ_{max} at 334 nm) because the octyloxy group, a weaker donor than the amino group, destabilizes less the HOMO which is centered on the styryl-donor moiety of the ligand. The same behavior was reported in literature for ligands having a similar structure but lacking the methyl groups at the 6 and 6' positions of the bipyridine.⁴⁹

Table 2. Absorption data for ligands **L1-L4** and of the complexes **C1-C5** recorded in CH_2Cl_2 .

λ (nm) [ϵ ($\text{M}^{-1}\text{cm}^{-1}$)]			
L1	393	[5.8×10^4]	C1
	310	[2.4×10^4]	
L2	399	[5.4×10^3]	C2
	272	[3.9×10^4]	
L3	401	[5.5×10^4]	C3

	296 [4.4×10^4]		285 [5.9×10^4]
			256 [5.0×10^4]
L4	334 [6.1×10^4]	C4	418 [4.8×10^4]
		C5	484 [1.1×10^4]
			344 [5.9×10^4]
			297 [5.1×10^4]
			253 [4.0×10^4]

The UV-Vis absorption spectra of the complexes **C1-C5** are characterized by two main contributions: a broad absorption band in the visible region corresponding to the charge-transfer (CT) transitions and a ligand-centered absorption band in the UV (Figure 4).

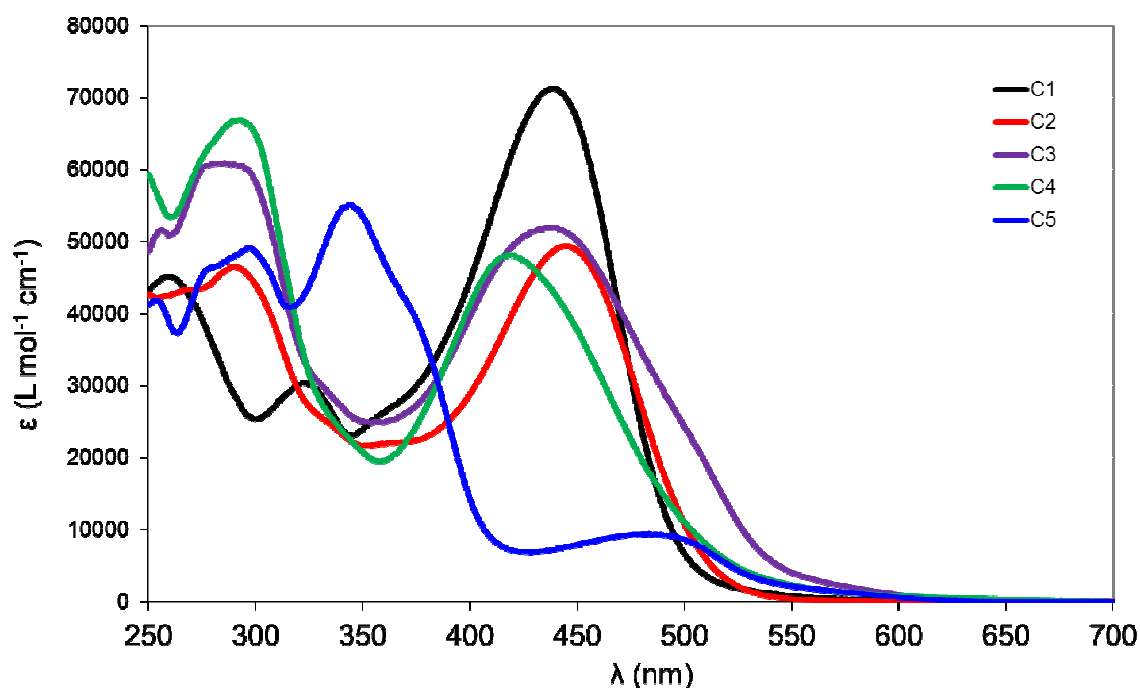


Figure 3. Normalized UV-Vis absorption spectra of the complexes **C1-C5** recorded in dichloromethane

The charge transfer bands of these complexes are very intense and exhibit absorption maxima ranging from 418 nm to 484 nm. Such an intense visible absorption band is very unusual for **DPEphos**-containing copper (I) complexes, whose spectra are normally limited to the UV region.^{7, 34, 35} High molar extinction coefficient values of the visible band ($\sim 5 \times 10^4 \text{ L mol}^{-1} \text{ cm}^{-1}$) constitute a marked improvement of the light absorbing properties of diimine Cu^{I} complexes. Indeed, the molar extinction coefficients of **C1-C5** are almost one order of magnitude higher than

those of regular copper(I) diimine complexes (for example $[\text{Cu}(\text{neocuproine})_2]^+$ $\epsilon = 8 \times 10^3 \text{ L mol}^{-1} \text{ cm}^{-1}$). The visible absorption band results from the superposition of several transitions corresponding to a mixture of metal to ligand charge transfers (MLCTs) and intraligand charge transfer (ILCT, see results of TD-DFT calculations in the computational study). The contribution of the intense styrylbipyridine ILCT transition is responsible for this impressive ϵ value, as the metal ion acts as an inductive acceptor by stabilizing the bipyridine-centred LUMO and provoking the red-shift of the band with respect to the free ligands.

Electrochemistry

The electrochemical properties of the ligands and of the complexes were measured in dichloromethane and all the potentials are referred to SCE reference electrode (**Table 3**). An irreversible wave around 0.64 V was attributed to the oxidation of the amines in **L1** which decompose according to a β -elimination reaction.⁵⁰ **L2** displays a first oxidation wave attributed to the removal of an electron from the amine units. This process is not reversible, probably because of the absence of a *para* substitution on the phenyl rings, which enables chemical reaction from the radical generated at this position. Indeed, in ligand **L3**, having donating methoxy groups in the *para* position, the oxidation process at 0.87 V is reversible. This potential is anodically shifted compared to **L1**, accounting for the less electron rich nature of diphenylamine with respect to diethylamine. No oxidation wave was recorded in **L4**, confirming that the weaker donating nature of the alkyloxy groups.

Table 3. Oxidation potentials of ligands **L1-L4** and of complexes **C1-C5** measured by square wave voltammetry in dichloromethane with 0.1 M TBAPF₆ as supporting electrolyte. Reference electrode: SCE. ^aIrreversible process. ^b Superimposed waves.

	E(amine ⁺ /amine) (V vs. SCE)	E(Cu ^{II} /Cu ^I) (V vs. SCE)
L1	0.64 ^a	—
L2	0.90 ^a 0.87	—
L3	0.87	—
L4	—	—
C1	0.73 ^a	1.32 ^a
C2	0.70	1.34
C3	0.71	0.87
C4	0.96 ^b	1.03 ^b
C5	—	0.80

The electrochemical properties of the complexes **C1-C5** were then investigated. The first complex, **C1**, shows a two-electron irreversible process assigned to oxidation of the diethylaminophenyl units. Complexes **C2-C4**, containing the aromatic tertiary amines, display a reversible two-electron oxidation wave around 0.7 V assigned to electron removal at the nitrogen of the amine substituents of the styryl moieties. A second one-electron oxidation reaction, attributed to the Cu^{II}/Cu^I couple, is then observed. Interestingly, the sterically more constrained coordination sphere in complex **C4** relative to **C3** and **C5** anodically shifts the oxidation potential of the Cu^{II}/Cu^I couple because the four aryl rings hinder the flattening of the tetrahedral complexes and destabilize the Cu^{II} state, which prefers a square planar environment. The **DPEphos** ligand induces an important anodic shift of the oxidation potential of Cu^{II}/Cu^I couple (see **C2 versus C3**), because it imposes a large steric hindrance around the metal and has a lower electron-donating effect compared to that of Mes₂Phen.^{11,12,14, 23} The cathodic behavior was also investigated, but nothing significantly different from the blank was observed until a potential of -1.5 V vs. SCE, which was the onset of solvent electroactivity in our conditions. This indicates that the first reduction processes (localized on the bipyridine portion of the diimine ligand according to TD-DFT calculations) occur at a more negative potential than -1.5 V vs. SCE both in the ligands and in the complexes.

Computational study

The Cartesian coordinates of the optimized structures are shown in SI (Table S3). The bond lengths of Cu-N(L) are about 2.09 Å for DPEPhos complexes (**C1-C2**) which are slightly longer than those of Mes₂Phen complexes (**C3-C5**) which range from 2.00 Å to 2.02 Å. The Cu-P(DPEPhos) bond lengths are 2.23-2.25 Å which are similar to those in crystal structure of [CuCl(DPEPhos)(dmpymtH)] complex (dmpymtH: 4,6-dimethylpyrimidine-2(1H)-thione), 2.2966 Å and 2.2829 Å.⁵¹ The bond lengths of Cu-N(Mes₂Phen) are 2.05-2.11 Å for the nitrogen near π -stacking Mes ligand while 1.99-2.02 Å for another nitrogen.

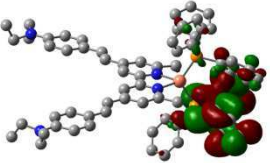
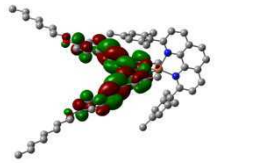
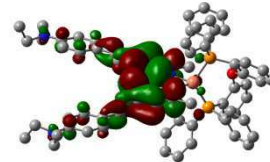
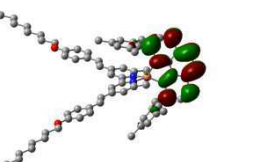
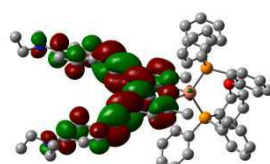
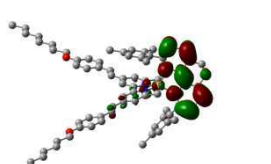
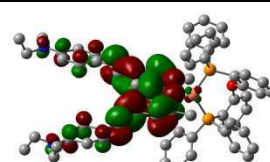
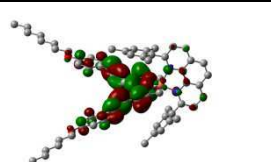
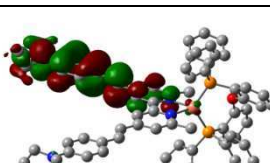
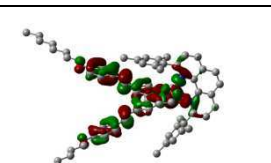
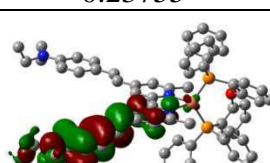
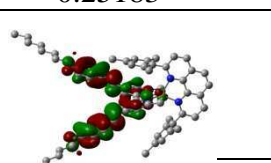
In order to get detailed understanding of the experimental electrochemical data reported above, we did perform a fragment analysis at PBE-D/TZP level.⁵² The complexes are separated into three fragments, that is, L, DPEPhos/Mes₂Phen, and Cu⁺, to see the contribution of KS orbitals of each fragment to those of the complexes. The HOMO of **C1** is mainly localized on **L1** (88 %), especially on aminostyryl moieties. The largest contributions come from two nitrogen atoms of amines (19 %). The ethyl substituents do not contribute to the HOMO. In **C2** and **C3**, the HOMO is localized on **L3** (97 % and 90 %, respectively) and mainly on aminostyryl moieties as in **C1**. The largest contributions come from two nitrogen atoms of amines (18 %) and from anisyl substituents (13 % and 12 %, respectively). In **C4**, the HOMO is also localized on **L2** (47 %) but with a large contribution from Cu (39 %). In **L2** fragment, two nitrogen atoms of amines contribute

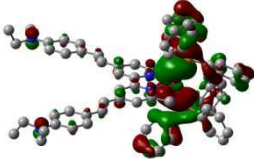
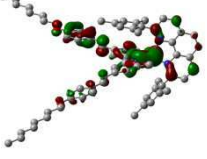
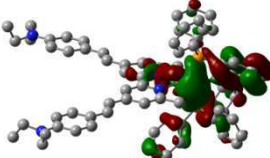
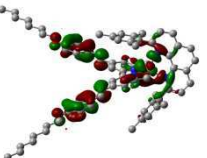
predominantly (9 %), the phenyl substituents contributing slightly (3 %). Comparing **C1** and **C2-C4**, we may observe a difference in the electronic distributions of the HOMO in the complexes. In **C1**, the HOMO is more localized because the ethyl substituents do not contribute significantly. The HOMO of **C2-C4** are more delocalized over substituted aminostyryl moieties. In contrast, the HOMO of **C5** is mainly localized on Cu (59 %) with significant contributions of **L4** (20 %) and diMesPhen (15 %). A large contribution of d orbitals of Cu fragment characterizes the HOMO-2 in **C1-C3**. The main contributions to the HOMO-2 in **C1** and **C2** are due to the Cu fragment (44 % and 38 %, respectively) with a large contribution of DPEPhos fragment (32 % and 35 %, respectively) and a moderate contribution of **L1** or **L2** (19 % and 23 %, respectively). On the other hand, HOMO-2 of **C3** is more concentrated on Cu (60 %) than in **C1** or **C2** with a contribution of diMesPhen (15 %) and **L3** (21 %). These theoretical analysis clearly indicates that in complexes **C1-C4**, the first oxidation process is ligand-based and more particularly it involves the amino group. Conversely, in complex **C5** copper center is strongly involved in the electron removal.

To get a better understanding of the absorption properties of this series of complexes and to determine the nature of the electronic transitions implied in the visible absorption band, Time-Dependent Density Functional Theory (TD-DFT) calculations were undertaken. For comparison the theoretical absorption spectra calculated in solvent are represented in Figure S1. The electronic density distribution of the frontier orbitals (from HOMO-3 to LUMO+3) is represented in Table S2 (all complexes) and Table 4 (complexes **C1** and **C5**). The calculated transition energies to the low-lying excited states of **C1-C5** and the dipole-allowed vertical absorption wavelength (λ , in nm) with their oscillator strengths (f) are listed in Table S1 (all complexes) and Table 5 (Complexes **C1** and **C5**). The energy of the frontier orbitals are reported in Figure 4. A qualitative analysis of the main contributions to the molecular orbitals, coupled with the data from the dipole-allowed transitions, provides useful information about the nature of the bands. The HOMO and HOMO-1 orbitals are mainly localized on the donor groups of the styryl ligand for all the complexes. In **C1-C4** these orbitals are nearly degenerate, and mainly localized on the two styryl branches of the ligands **L1-L3**. The HOMO of **C5**, on the contrary, additionally contains a strong contribution of copper, and lies at lower energy (Figure 4). This is clearly an effect of the reduced electron donating character of the *n*-octyloxy group with respect to aliphatic and aromatic amines, and corroborates the above observations. This translates in the oxidation potential of complex **C5**, which is essentially a copper based process and is anodically shifted relative to that of complex **C3** which is a ligand based process (Tables 3&4). The HOMO-2 and HOMO-3 have different characters depending on the nature of the bulky ligand. They are essentially metal-based orbitals with some contribution of the styryl ligand for diimine complexes (**C3**, **C4** and **C5**), whereas they are delocalized over the metal

and phosphines for complexes with **DPEphos** (**C1** and **C2**), in agreement with literature data.⁵³⁻⁵⁵ Besides, the energy spacing between HOMO-1 and HOMO-2 is larger for bisphosphine complexes while it is weaker in bisdiimine complexes. On the other hand, the LUMO and LUMO+1 are localized on the pyridyl moieties of styryl bipyridine for mixed [Cu(P[^]P)(N[^]N)]PF₆ complexes, while in bisdiimine complexes the LUMO+1 is fully localized on **L1** and its energy is close to the LUMO (fully residing on the styryl bipyridine). These differences in the localization of the molecular orbital translate into the nature of the transitions occurring in the visible region (Table S2 and Table 4).

Table 4. Graphical representation of the optimized structure and frontier molecular orbitals (from HOMO-3 to LUMO+3) of the copper (I) complexes **C1** and **C5** calculated using CAM-B3LYP functional considering solvent effect of dichloromethane with their energies in atomic unit.

L+3	 -0.00979	 -0.03600
L+2	 -0.01152	 -0.04174
L+1	 -0.03380	 -0.04666
L	 -0.05723	 -0.05588
H	 -0.23755	 -0.25183
H-1	 	

	-0.23817	-0.26121
H-2	 -0.27335	 -0.26425
H-3	 -0.29572	 -0.27341
	C1	C5

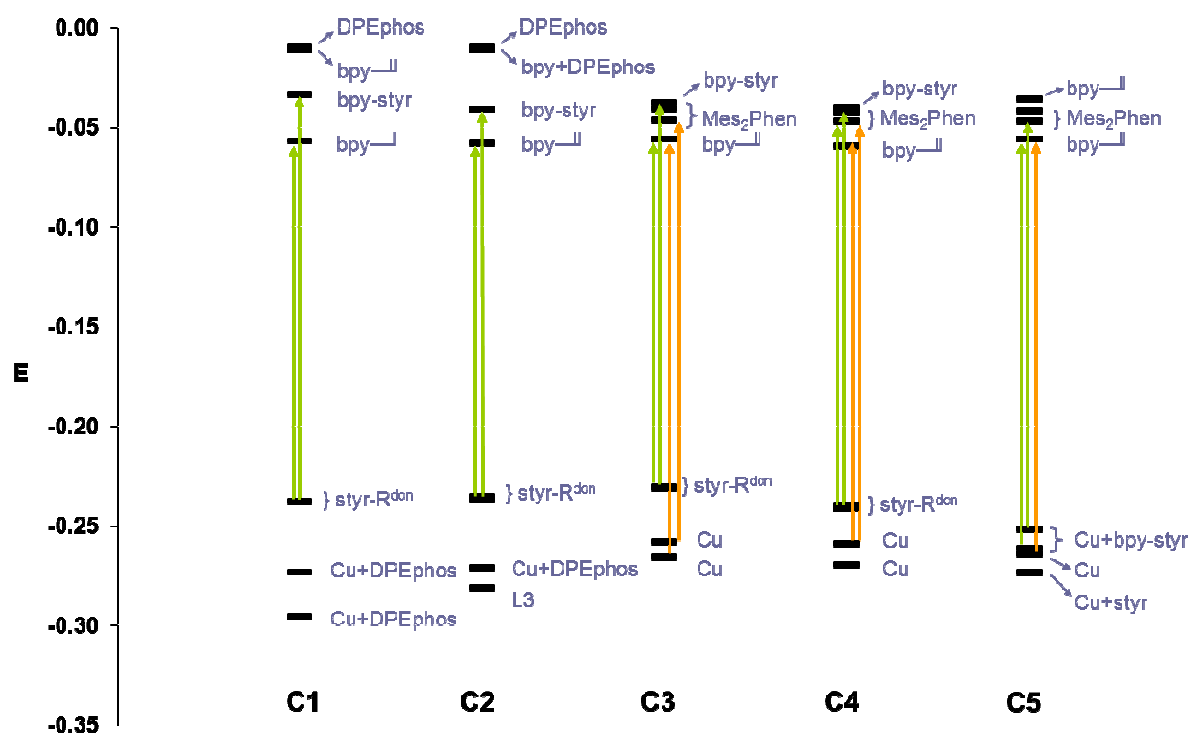


Figure 4. Energy diagram of the frontier orbitals of complexes **C1-C5**. The energy (E) is given in a.u.. Each KS orbital is labelled by the most significant contributing fragment. The arrows indicate the electronic transitions responsible for the visible absorption: ILCTs (intra-ligand charge transfer) are represented in green and MLCTs (metal-to-ligand charge transfer) in orange. Bpy—|| indicates the bipyridine plus the double bond of the styryl group.

The TD-DFT (CAM-B3LYP) transition energies (in nm) to the low-lying singlet excited states of complexes **C1-C5** and associated oscillator strengths f calculated in dichloromethane are

reported in Table S1 and Table 5. In the **DPEphos substituted** complexes (**C1** and **C2**), the absorption band around 440 nm corresponds to a mixture of pure ILCT transitions, namely a displacement of electronic density from the donor group to the bipyridyl subunit of the styryl bipyridine ligand. The lowest MLCT absorption bands are calculated in the near UV with weak oscillator strengths, and assigned to a mixed MLCT/ILCT state with more than 70% of MLCT character (see SI for the detail of transition wavelengths and oscillator strengths). This is the consequence of the low lying position of the filled copper orbital (HOMO-3) that is due to the lower σ -donating strength of the phosphine compared to the diimine ligand. The interest in using conjugated styryl-bipyridine ligands is evidenced by the fact that the LUMOs are centred on the bipyridine core plus the double bond or the entire styryl moiety. The extended conjugation of the π system, compared to simple bipyridine or alkyl-bipyridine ligands, contributes to the red-shift of the absorption bands.

Table 5. TD-DFT (CAM-B3LYP) transition energies (in nm) to selected low-lying singlet excited states of complexes **C1** and **C5** and associated oscillator strengths f calculated in dichloromethane. The main character of the state is given in percentage (in parenthesis).

complex	state	ΔE (nm)	f
C1	ILCT _{L1} (94%)	410	1.37
	ILCT _{L1} (90%)	397	1.95
	MLCT _{L1} (72%) / ILCT _{L1} (14%)	325	0.07
	ILCT _{L1} (92%)	310	0.08
	ILCT _{L1} (67%) / MLCT _{L1} (22%)	299	0.23
	ILCT _{L1} (83%)	291	0.26
	ILCT _{L1} (39%) / MLCT _{L1} (34%)	257	0.11
C5	MLCT _{Mes2Phen} (53%) / MLCT _{L4} (38%)	447	0.12
	MLCT _{L4} (56%) / MLCT _{Mes2Phen} (32%)	421	0.10
	MLCT _{L4} (45%) / MLCT _{Mes2Phen} (43%)	395	0.42
	ILCT _{L4} (52%) / MLCT _{L4} (34%)	362	1.48
	MLCT _{Mes2Phen} (52%) / MLCT _{L4} (33%)	359	0.07
	MLCT _{L4} (26%) / ILCT _{Mes2Phen} (24%) / LLCT _{L4} (19%) / ILCT _{L4} (13%)	332	0.45
	ILCT _{Mes2Phen} (40%) / MLCT _{L4} (26%) / ILCT _{L4} (14%)	330	0.43
	LLCT _{L4} (40%) / MLCT _{Mes2Phen} (13%) / ILCT _{Mes2Phen} (11%) / MLCT _{L4} (10%)	306	0.14

	ILCT _{Mes2Phen} (70%) / MLCT _{Mes2Phen} (16%)	275	0.10
	ILCT _{Mes2Phen} (52%)	271	0.26
	ILCT _{L4} (41%) / LLCT _{L4} (21%) / MLCT _{L4} (13%)	264	0.24
	ILCT _{Mes2Phen} (55%)	251	0.20

In heteroleptic bis-diimine complexes (**C3**, **C4** and **C5**), the absorption band in the visible is assigned to distinct transitions corresponding to MLCTs and ILCT states calculated between ~ 440 nm and ~ 370 nm with significant oscillator strengths. Interestingly, there are two MLCTs transitions: the main one involves the Mes₂Phen and its oscillator strength is twice more intense than the one involving the styryl bipyridine (SI). However, the high energy side of the visible band is dominated by an intense ILCT transition, which is certainly mostly responsible for the high extinction coefficient of the complexes in this region. The strongest calculated peak locates around 400 nm for **C1-C4** while around 360 nm for **C5**. Logically, the position of this transition is proportional to the strength of the electron releasing group on the styryl moiety and naturally decreases in the following order N(Et)₂ > N(Anysyl)₂ ≈ N(Ph)₂ >> OOctyl. In the spectrum of **C5**, even the low energy bands formally assigned to ILCT transitions contain the contribution of copper (I) to the electron density of the departure orbital, thus having a partial MLCT character. Another distinction of the spectra of the diimine complexes is the presence of a small absorption tail above 430 nm, attributed to band I according to the nomenclature of Ichinaga and co-workers⁵⁶ and which is typical of a flattened complex. The flattening is caused by the π-stacking interactions of the mesityl groups with the bipyridine and this raises the energy of the d_{yz} upon bending of **L1** in the xz plane.

Conclusions

In this study a series of five new heteroleptic copper(I) complexes were designed with the aim of improving the visible absorption properties of this class of compounds, which are, at the present time, one of the limitations for their use in solar energy conversion. To reach this goal, chromophoric styrylbipyridine ligands were introduced in the coordination sphere. Bulky dimesitylphenanthroline and **DPEphos** were chosen as complementary ligands. These series of complexes exhibit indeed very intense absorption bands ($5\text{-}7 \times 10^4 \text{ M}^{-1}\text{cm}^{-1}$) in the visible. The analysis of the position, intensity and band shape, which are rationalized with the help of TD-DFT calculations, indicates a strong contribution of an intra-ligand charge-transfer transition centered on the styrylbipyridine ligand along with MLCT transitions. The analysis of the main contributions to the absorption in the visible region of the spectrum unveils that intra-ligand charge transfer transitions

play a major role. This fact could cause important consequences on the emission properties, as all the considerations made until now on the luminescence properties of copper(I) complexes are based on emission from MLCT states. Work in this direction is currently underway in our laboratories.

Reference

1. S. Campagna, F. Puntoriero, F. Nastasi, G. Bergamini and V. Balzani, *Top. Curr. Chem.*, 2007, **280**, 117-214.
2. D. Kumaresan, K. Shankar, S. Vaidya and R. H. Schmehl, *Top. Curr. Chem.*, 2007, **281**, 101-142.
3. J. A. G. Williams, *Top. Curr. Chem.*, 2007, **281**, 205-268.
4. L. Flamigni, A. Barbieri, C. Sabatini, B. Ventura and F. Barigelletti *Top. Curr. Chem.*, 2007, **281**, 143-203.
5. R. Kirgan, B. P. Sullivan and D. P. Rillema, *Top. Curr. Chem.*, 2007, **281**, 45-100.
6. N. Armaroli, *Chem. Soc. Rev.*, 2001, **30**, 113-124.
7. N. Armaroli, G. Accorsi, F. Cardinali and A. Listorti, *Top. Curr. Chem.*, 2007, **280**, 69-115.
8. M. T. Miller, P. K. Gantzel and T. B. Karpishin, *Inorg. Chem.*, 1998, **37**, 2285-2290.
9. A. Lavie-Cambot, M. Cantuel, Y. Leydet, G. Jonusauskas, D. M. Bassani and N. D. McClenaghan, *Coord. Chem. Rev.*, 2008, **252**, 2572-2584.
10. M. T. Miller, P. K. Gantzel and T. B. Karpishin, *J. Am. Chem. Soc.*, 1999, **121**, 4292-4293.
11. N. A. Gothard, M. W. Mara, J. Huang, J. M. Szarko, B. Rolczynski, J. V. Lockard and L. X. Chen, *J. Phys. Chem. C*, 2012, **116**, 1984-1992.
12. Q. Zhang, Q. Zhou, Y. Cheng, L. Wang, D. Ma, X. Jing and F. Wang, *Adv. Funct. Mater.*, 2006, **16**, 1203-1208.
13. G. Che, Z. Su, W. Li, B. Chu, M. Li, Z. Hu and Z. Zhang, *Appl. Phys. Lett.*, 2006, **89**, 103511.
14. O. Moudam, A. Kaeser, B. Delavaux-Nicot, C. Duhayon, M. Holler, G. Accorsi, N. Armaroli, I. Seguy, J. Navarro, P. Destruel and J.-F. Nierengarten, *Chem. Commun.*, 2007, **0**, 3077-3079.
15. C. S. Smith, C. W. Branham, B. J. Marquardt and K. R. Mann, *J. Am. Chem. Soc.*, 2010, **132**, 14079-14085.
16. L. Shi, B. Li, S. Lu, D. Zhu and W. Li, *Appl. Organomet. Chem.*, 2009, **23**, 379-384.
17. T. Bessho, E. C. Constable, M. Graetzel, A. Hernandez Redondo, C. E. Housecroft, W. Kylberg, M. K. Nazeeruddin, M. Neuburger and S. Schaffner, *Chem. Commun.*, 2008, 3717-3719.
18. B. Bozic-Weber, E. C. Constable, C. E. Housecroft, P. Kopecky, M. Neuburger and J. A. Zampese, *Dalton Trans.*, 2011, **40**, 12584-12594.
19. B. Bozic-Weber, E. C. Constable, C. E. Housecroft, M. Neuburger and J. R. Price, *Dalton Trans.*, 2010, **39**, 3585-3594.
20. E. C. Constable, A. H. Redondo, C. E. Housecroft, M. Neuburger and S. Schaffner, *Dalton Trans.*, 2009, 6634-6644.
21. S.-P. Luo, E. Mejía, A. Friedrich, A. Pazidis, H. Junge, A.-E. Surkus, R. Jackstell, S. Denurra, S. Gladiali, S. Lochbrunner and M. Beller, *Angew. Chem. Int. Ed.*, 2013, **52**, 419-423.
22. H. Akdas-Kilig, J.-P. Malval, F. Morlet-Savary, A. Singh, L. Toupet, I. Ledoux-Rak, J. Zyss and H. Le Bozec, *Dyes Pigments*, 2012, **92**, 681-688.
23. C. L. Linfoot, P. Richardson, T. E. Hewat, O. Moudam, M. M. Forde, A. Collins, F. White and N. Robertson, *Dalton Trans.*, 2010, **39**, 8945-8956.
24. T. Renouard, H. Le Bozec, S. Brasselet, I. Ledoux and J. Zyss, *Chem. Commun.*, 1999, 871-872.
25. M. Schmittel and A. Ganz, *Chem. Commun.*, 1997, 999-1000.

26. O. Maury, L. Viau, K. Sénéchal, B. Corre, J.-P. Guégan, T. Renouard, I. Ledoux, J. Zyss and H. Le Bozec, *Chem. Eur. J.*, 2004, **10**, 4454-4466.
27. A. P. Smith, J. J. S. Lamba and C. L. Fraser, *Org. Synth.*, 2002, **78**, 82-87.
28. A. Listorti, G. Accorsi, Y. Rio, N. Armaroli, O. Moudam, A. Gegout, B. Delavaux-Nicot, M. Holler and J.-F. Nierengarten, *Inorg. Chem.*, 2008, **47**, 6254-6261.
29. S. Grimme, *J. Comput. Chem.*, 2006, **27**, 1787-1799.
30. M. Pirtsch, S. Paria, T. Matsuno, H. Isobe and O. Reiser, *Chem.- Eur. J.*, 2012, **18**, 7336-7340.
31. S. De, K. Mahata and M. Schmittel, *Chem. Soc. Rev.*, 2010, **39**, 1555-1575.
32. C. Lee, J.-H. Yum, H. Choi, S. Ook Kang, J. Ko, R. Humphry-Baker, M. Grätzel and M. K. Nazeeruddin, *Inorg. Chem.*, 2007, **47**, 2267-2273.
33. P. Wang, C. Klein, R. Humphry-Baker, S. M. Zakeeruddin and M. Grätzel, *J. Am. Chem. Soc.*, 2004, **127**, 808-809.
34. D. G. Cuttell, S.-M. Kuang, P. E. Fanwick, D. R. McMillin and R. A. Walton, *J. Am. Chem. Soc.*, 2002, **124**, 6-7.
35. N. Armaroli, G. Accorsi, M. Holler, O. Moudam, J. F. Nierengarten, Z. Zhou, R. T. Wegh and R. Welter, *Adv. Mater.*, 2006, **18**, 1313-1316.
36. M. Schmittel, U. Lüning, M. Meder, A. Ganz, C. Michel and M. Herderich, *Heterocyclic Commun.*, 1997, **3**, 493.
37. H. Nitadori, L. Ordroneau, J. Boixel, D. Jacquemin, A. Boucekkine, A. Singh, M. Akita, I. Ledoux, V. Guerchais and H. Le Bozec, *Chem. Commun.*, 2012, **48**, 10395-10397.
38. S. Karlsson, J. Boixel, Y. Pellegrin, E. Blart, H.-C. Becker, F. Odobel and L. Hammarström, *J. Am. Chem. Soc.*, 2010, **132**, 17977-17979.
39. G. J. Kubas, B. Monzyk and A. L. Crumblis, in *Inorg. Synth.*, John Wiley & Sons, Inc., 2007, pp. 68-70.
40. E. Van Lenthe and E. J. Baerends, *J. Comput. Chem.*, 2003, **24**, 1142-1156.
41. Z. He, C. Zhong, X. Huang, W.-Y. Wong, H. Wu, L. Chen, S. Su and Y. Cao, *Adv. Mater.*, 2011, **23**, 4636-4643.
42. M. Kayanuma, N. Bera, M. Sandroni, Y. Pellegrin, E. Blart, F. Odobel and C. Daniel, *C. R. Chimie*, 2012, **15**, 255-266.
43. M. Petersilka, U. J. Gossmann and E. K. U. Gross, *Phys. Rev. Lett.*, 1996, **76**, 1212.
44. T. Yanai, D. Tew and N. Handy, *Chem. Phys. Lett.*, 2004, **393**, 51.
45. J. Tomasi, B. Mennucci and R. Cammi, *Chem. Rev.*, 2005, **105**, 2999.
46. N. C. Bera, I. Bhattacharyya and A. K. Das, *Spectrochim. Acta, Part A*, 2007, **67A**, 894.
47. T. H. Dunning, Jr., *J. Chem. Phys.*, 1989, **90**, 1007.
48. Frisch, M. J.; Trucks, G. W.; Schlegel, H. B.; Scuseria, G. E.; Robb, M. A.; Cheeseman, J. R.; Scalmani, G.; Barone, V.; Mennucci, B.; Petersson, G. A.; Nakatsuji, H.; Caricato, M.; Li, X.; Hratchian, H. P.; Izmaylov, A. F.; Bloino, J.; Zheng, G.; Sonnenberg, J. L.; Hada, M.; Ehara, M.; Toyota, K.; Fukuda, R.; Hasegawa, J.; Ishida, M.; Nakajima, T.; Honda, Y.; Kitao, O.; Nakai, H.; Vreven, T.; Montgomery J. A. Jr.; Peralta, J. E.; Ogliaro, F.; Bearpark, M.; Heyd, J. J.; Brothers, E.; Kudin, K. N.; Staroverov, V. N.; Keith, T.; Kobayashi, R.; Normand, J.; Raghavachari, K.; Rendell, A.; Burant, J. C.; Iyengar, S. S.; Tomasi, J.; Cossi, M.; Rega, N.; Millam, J. M.; Klene, M.; Knox, J. E.; Cross, J. B.; Bakken, V.; Adamo, C.; Jaramillo, J.; Gomperts, R.; Stratmann, R. E.; Yazyev, O.; Austin, A. J.; Cammi, R.; Pomelli, C.; Ochterski, J. W.; Martin, R. L.; Morokuma, K.; Zakrzewski, V. G.; Voth, G. A.; Salvador, P.; Dannenberg, J. J.; Dapprich, S.; Daniels, A. D.; Farkas, O.; Foresman, J. B.; Ortiz, J. V.; Cioslowski, J.; Fox, D. J.; *Gaussian 09, Revision B.01*; Gaussian, Inc.: Wallingford, CT, 2010.

49. O. Maury, J.-P. Guegan, T. Renouard, A. Hilton, P. Dupau, N. Sandon, L. Toupet and H. L. Bozec, *N. J. Chem.*, 2001, **25**, 1553-1566.
50. R. Ziessel, A. Juris and M. Venturi, *Inorg. Chem.*, 1998, **37**, 5061-5069.
51. P. Aslanidis, P. J. Cox and A. C. Tsipis, *Dalton Trans.*, 2010, **39**, 10238-10248.
52. G. te Velde, F. M. Bickelhaupt, E. J. Baerends, C. Fonseca Guerra, S. J. A. van Gisbergen, J. G. Snijders and T. Ziegler, *J. Comp. Chem.*, 2001, **22**, 931-967.
53. L. Yang, J.-K. Feng, A.-M. Ren, M. Zhang, Y.-G. Ma and X.-D. Liu, *Eur. J. Inorg. Chem.*, 2005, **2005**, 1867-1879.
54. L.-Y. Wang, Y. Xu, Z. Lin, N. Zhao and Y. Xu, *J. Luminescence*, 2011, **131**, 1277-1282.
55. C. Wen, G. Tao, X. Xu, X. Feng and R. Luo, *Spectrochim. Acta A Mol. Biomol. Spectros.*, 2011, **79**, 1345-1351.
56. A. K. Ichinaga, J. R. Kirchhoff, D. R. McMillin, C. O. Dietrich-Buchecker, P. A. Marnot and J. P. Sauvage, *Inorg. Chem.*, 1987, **26**, 4290-4292.